Chapter 18
Rock Mass Classification of Chalk Marl in the UK Channel Tunnels Using *Q*

Nick Barton and Colin Warren

18.1 Introduction

The Channel Tunnel was driven in chalk marl with the prior expectation by the designers of quite ideal tunnelling conditions on the UK side. This expectation was partly the result of little emphasis on the implications of joint structure. As a result of the difficulties and initial delays caused by overbreak in some of the UK sub-sea TBM drives, the first author was requested to assess the rock quality in existing tunnels in chalk marl. The work was performed during 1990 and 1991 under contract to GeoEngineering who were conducting a major review for Eurotunnel. The assessment was made using the *Q*-system of rock mass classification (Barton et al. 1974) which was also being used by TransManche Link (TML) in the Marine Service and Running Tunnels. The first author's classification of the grey chalk at Shakespeare Cliffs and of the chalk marl in the Beaumont and Terlingham Tunnels was performed prior to any data being provided on conditions in the Marine Service Tunnel (MST) or in the Marine Running Tunnel (MRT). The PB series of core logs and photographs for marine drill core PB1 to PB8 was also classified without prior knowledge of MST or MRT conditions. The extensive MST and MTR *Q*-logging by TML was subsequently made available by the second author of this paper, who was Eurotunnel's chief geologist. The comparison of multiple parties' *Q*-logging was satisfactorily close.

N. Barton (✉)
Nick Barton & Associates – Formerly Norwegian Geotechnical Institute, Oslo, Norway

C. Warren
Warren Geotechnical Associates, Surrey, UK – formerly Sir William Halcrow and Partners, London, UK

© Springer Nature Switzerland AG 2020

M. Kanji et al. (eds.), *Soft Rock Mechanics and Engineering*,
https://doi.org/10.1007/978-3-030-29477-9_18

TransManche Link TML's own rock mass *Q*-characterisation in the Marine Service Tunnel for km 20–30 was based on 250 face logs and 1120 side wall logs. Average *Q*-values were 9.9 for km 20–24 where most ring-building difficulties with overbreak were experienced above the cutter-head and shield, and *Q* averaged 33.4 for km 24–30. Lower values were obtained when only face logs were analysed, due to the absence of swarf. In the low cover zone from km 20.5 to 21.3, TML's mean *Q*-value was only 5.6. The above range of mean *Q*-values is very similar to that obtained independently from the pre-construction sources by the first author. According to *Q*-system case records, tunnels of 8.4 m span (two Marine Running Tunnels, MRT) and 5.3 m span (Marine Service Tunnel, MST) need *Q*-values of 40 and 10 respectively for no support to be required. The 17–18 m of unsupported tunnel lengths behind the MST and MRT tunnel boring machine tunnel faces made overbreak a very likely phenomenon when *Q*-values were in the range 1–10. (Sharp et al. 1996). Since rock mass classification is very much based on visual assessment and experience, it is judged to be helpful if the following chalk and chalk marl classifications are illustrated by some representative photographs. The starting point is logically the overlying grey chalk at Shakespeare Cliffs which is illustrated in Fig. 18.1.

Fig. 18.1 Left: Representative conjugate jointing and sub-horizontal bedding in the grey chalk at Shakespeare Cliffs. Right: Joints in the underlying chalk marl where the tunnels were to be constructed. Note the extreme planarity of the joints, which was responsible for extensive overbreak in permeable, lower-cover sections

18.2 *Q*-classification of Grey Chalk at Shakespeare Cliffs

The strongly developed bedding and steeply dipping conjugate jointing are easily recognised at many locations along the cliffs. Figure 18.1 is a typical illustration of joints, with the bedding less clearly seen. Superficial (non-systematic) *Q*-system classification of the grey chalk exposed in the lower cliffs gave the following preliminary indications of potential rock mass quality, where *Q* is defined as:

$$RQD / J_n \times J_r / J_a \times J_w / SRF \tag{18.1}$$

1. Typical $Q = (80–90)/9 \times 2/1 \times 1/1 = 18–22$ (good)
2. Range $Q = (70–100)/(6–12) \times (1.5–2)/(1–2) \times 1/1 = 4.4–33$ (fair to good)

These parameters describe RQD (rather high); J_n, number of joint sets (often three); J_r, roughness (smooth undulating); J_a, alteration (not visible); J_w, water inflow (optimistically low) and SRF, stress/strength (assumed favourable). The degree to which the observed jointing was representative of jointing in the chalk marl was examined in much more detail in relation to marine drill core and in underground exposures logged in the Beaumont and Terlingham Tunnels.

The steeply dipping and very persistent and planar WNW-ESE trending dominant joints seen both in the cliffs and in the chalk marl in the foreshore at low tide below the cliffs had virtually no undulation or small scale roughness. Measurements of amplitude/length (*a*/*L*) indicated very low values of joint roughness coefficient (JRC) (Barton and Choubey 1977) for these dominant steeply dipping joints. Shear strength would be correspondingly low. The significance of JRC values as low as 1–2 (more or less non-dilatant surfaces) for the stability of blocks in the periphery of a tunnel can be readily demonstrated in distinct element models such as UDEC and UDEC-BB (Cundall 1980; Makurat et al. 1990; Barton 1993). Today (Barton 2007 and more recently) we know that overbreak is inevitable when the ratio $J_n/J_r \geq 6$. In the present case, J_n/J_r was frequently 9/1.0 (three sets, smooth planar).

18.3 *Q*-classification of PB Series Drill Core

Potential tunnelling conditions in the chalk marl were assessed from Channel Tunnel marine drill core (PB series), and from direct classification of the chalk marl in the Beaumont and Terlingham Tunnels. In each case, the *Q*-parameters were logged in histogram format, to give a fair indication of the range of parameter values. An example of jointing in one of the PB1 to PB8 drill core is shown in Fig. 18.2.

Several hundred core box photographs and corresponding core logs and "fracture logs" were studied, resulting in the extensive set of histograms shown in Fig. 18.3. The six *Q*-parameters are shown on the left-hand side, with complementary estimates or measurements of joint frequency, spacing, joint roughness and joint wall strength on the right-hand side (see Barton et al. 1992a, b for a fuller description of

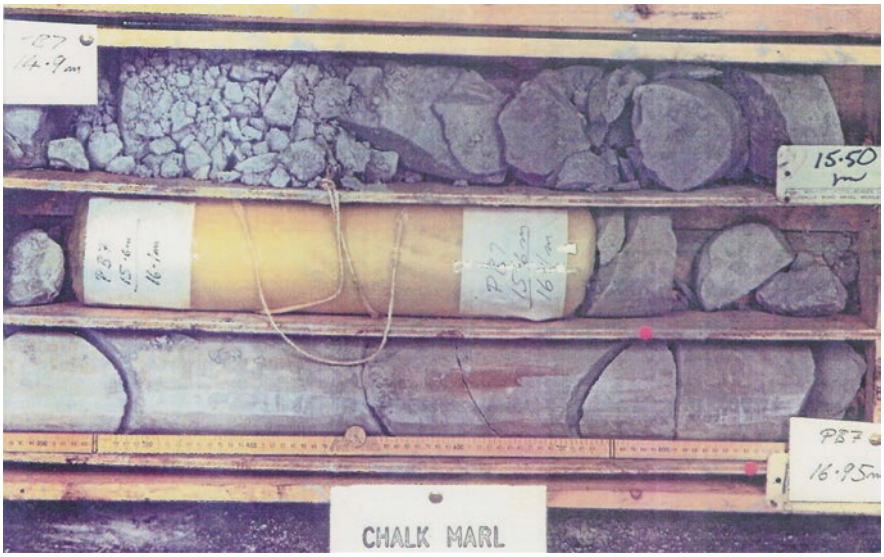

Fig. 18.2 Photograph of PB7 drill core, depth 14.9–16.95 m. Note three joint orientations

this geotechnical logging format). The jointing seen in Fig. 18.2 was described as follows at the time:

PB7: well jointed zone at 15–18 m in Chalk Marl. Joint surfaces are reportedly slickensided (i.e. J_r = 0.5–1.5 depending on planarity, J_n = 9 (or more), RQD = 85% (logged)).

The weighted mean sample for the six Q-parameters plotted in histogram form in Fig. 18.3 was as follows:

$$Q \text{ (mean)} = 89/6 \times 1.4/1.1 \times 0.8/1.2 = 12.6$$

Note in particular the low estimates of joint roughness JRC at core scale: JRC = 1–2 for bedding joints, and JRC = 2–3 for steeply dipping joints, and the correspondingly small roughness amplitudes (a/L at 10 cm scale; $a \approx 0.2$–1.0 mm).

18.4 *Q*-classification in the Terlingham and Beaumont Tunnels

Many hours were spent in Q-mapping and photography of the partly flooded Terlingham and Beaumont Tunnels. Areas of major overbreak and consistent breakage to sub-horizontal bedding planes *via* steeply dipping joints were a common feature in both tunnels. Examples of joint-related overbreak are shown in Fig. 18.4a–c. In some locations, many cubic metres of collapsed roof debris had to be climbed over, and it could be reasonably claimed that the tunnel cross-section had moved upwards (and outwards) a metre or so. The sub-horizontal bedding planes tended to

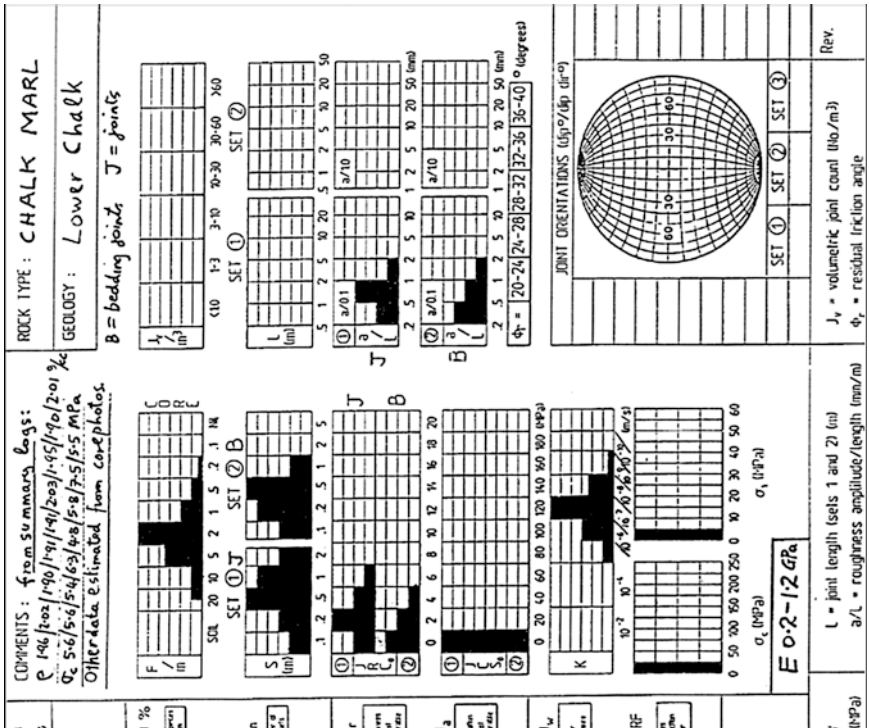

Fig. 18.3 Geotechnical and *Q*-characterisation of PB series drill core (PB1 through PB8)

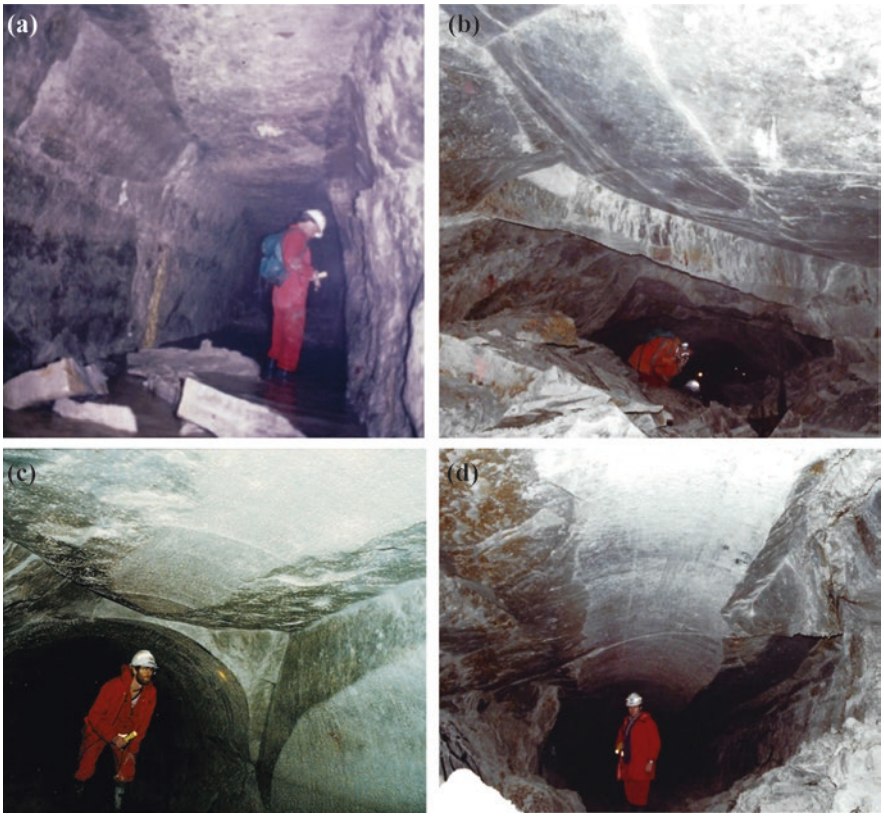

Fig. 18.4 (**a**, **b**) Joint and bedding plane controlled overbreak in Terlingham Tunnel and in Beaumont Tunnel. Some of the 2.2 m diameter tunnel can be seen in the background in (**b**). (**c**) The wedge fall-out in Beaumont Tunnel is joint controlled, as experienced at various scales in the MST and MRT tunnels, especially along ch. 20–24 km. (**d**) The effect of a local increase in depth of cover when passing under the 70 m high Shakespeare cliffs

form the new roof. They could be continuous for many tens of metres in places. The thousands of tidal cycles during the 110 years since 1880, may have been the cause of "arch migration" at Beaumont, where it ran beneath the tidal range.

There was also an "early chainage" stress-or-strain related fractured area, where the tunnel had passed under the cliffs, causing increased tangential stress and Poisson ratio related strain. (This is known from recent studies by Dr Baotang Shen using FRACOD: Barton and Shen 2017.) The stress-or-strain related fracturing is shown in Fig. 18.4d.

The Q-parameter histograms for the two tunnels are reproduced in Fig. 18.5.
Terlingham Tunnel: Q (mean) = 90/7.4 × 1.6/1.1 × 0.9/1.5 = 10.6
Q (typical range) = 1.3–50
Beaumont Tunnel: Q (mean) = 93.6/4.8 × 1.4/2.7 × 0.7/2.1 = 3.4
Q (typical range) = 0.2–100

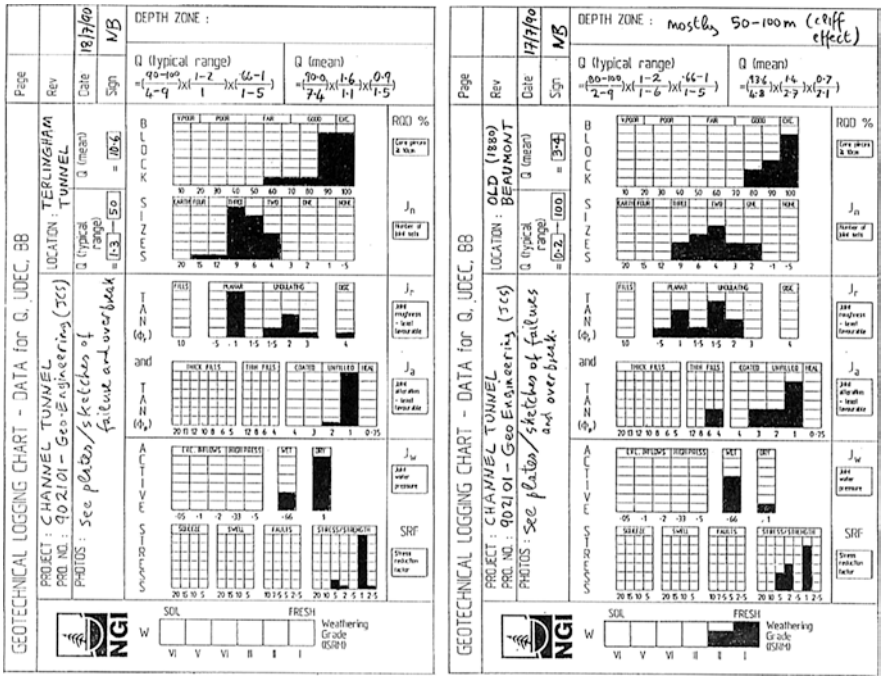

Fig. 18.5 *Q*-classification of the Terlingham and Beaumont (Abbots Cliff) Tunnels using histogram logging

The *Q*-parameter histogram method of logging used in Fig. 18.3 (see left side), was developed during air-travel to 50 km of headrace tunnels in Turkey, where much of the *Q*-logging had to be done from a jeep in motion, looking at countless road cuttings. This method of *Q*-parameter logging can clearly be used rapidly when needed, with sufficient practice. It was subsequently expanded, as in Fig. 18.3, to include other parameters needed for numerical DEM modelling during the UK Nirex LLW and ILW nuclear waste disposal project, 1990–1996, when 11 km of deep boreholes were *Q* (and sometimes RMR) logged in preparation for extensive UDEC-BB distinct element modelling of potential disposal cavern behaviour (Barton et al. 1992b).

The mapped section of the Beaumont tunnel had an overburden increasing under the cliffs from about 50–120 m. This resulted in some stress, or Poisson ratio extension-strain related failure in the haunches, which is reflected in the lower *Q*-values. In the case of the MST and MRT channel tunnels, the effective stress level caused by 20–60 m of rock cover and 30–50 m of sea depth is lower than some of Beaumont. Considering the uniaxial strength of the Chalk Marl (3.5–11 MPa, mean 6 MPa) the ratio of maximum principal stress to uniaxial strength (σ_θ/σ_c) lies well within the *Q*-system data base. Figure 18.4d illustrates part of this long (40–50 m) fractured zone.

18.5 Synthesis of *Q*-parameters from Precedent Data

Figure 18.3 shows the *Q*-system classification that was performed on PB1 to PB8 cores (using photos and logs). For comparison between the three sets of *Q*-parameter logging, Fig. 18.5 shows the *Q*-logging histograms for the Terlingham and Beaumont tunnels. The individual histograms have been combined in terms of relative frequency in Fig. 18.6. Numbers of observations are given from each mapping site so that a weighted mean can be obtained from the whole sample. The letters SH, BT, TT and PB refer respectively to Shakespeare Cliffs, Beaumont and Terlingham tunnels, and PB drill core.

Combining data from the four sites is considered important since the core logging may provide an overly optimistic picture of the joint frequency, as vertical holes were used. It is also valuable that the logging data could be tempered by the actual tunnelling experiences gleaned from inspection of the Beaumont and Terlingham tunnels. The addition of a very small number of observations in the grey chalk at Shakespeare Cliffs adds little to the data base. However, the experience of the jointing at the cliffs and along the foreshore is considered an important calibration process. With only moderate reduction in mechanical strength, it is inconceivable that jointing observed in the grey chalk at the Shakespeare Cliffs does not also penetrate the chalk marl in general, as indeed observed in these precedent tunnels, and in the foreshore below the cliffs (Fig. 18.1, Left). A synthesis of all the first author's *Q*-system observations from these sources resulted in the range of properties which were expected to apply to the MST and MRT drives under the Channel, shown in Fig. 18.6.

The rounded values (one decimal place accuracy) shown in Table 18.1 give a mean *Q* of 8.3. Rigorous multiplication and division of the whole (unrounded) sample gives a mean *Q* of 7.8. For practical purposes a round figure of $Q = 8$ can be adopted. The typical *range* of *Q* was 2–50 (poor to very good).

The suggested weighted mean of $Q = 8$ may not be the most typical or frequently occurring rock mass character. A glance at the histograms in Fig. 18.6 indicates that the following are the most frequently occurring characteristics according to the classifications performed:

1. Most frequent $Q = 100/9 \times 1/1 \times 1/1 = 11.1$
2. Next most frequent $Q = 90/4 \times 2/2 \times 0.66/2 = 7.4$
3. *Possible problem ground* $Q = 90/9 \times ½ \times 0.66/1 = 3.3$

A probable frequently occurring combination of the first two "classes", due to the likelihood of higher water inflows and slight joint alteration when three (as opposed to two) joint sets are present is given as *problem ground* #3. The 1993 updated version of the *Q*-system tunnel support diagram (Grimstad and Barton 1993), which is reproduced in Fig. 18.7, indicates that *Q*-values of approximately 40, 10 and 1 are required for permanent unsupported spans (diameters) of 8.4 m, 5.3 m and 2.1 m (i.e. the diameters for MRT, MST and Beaumont) respectively. The fact that some 40–50% of the Beaumont tunnel is still standing with its

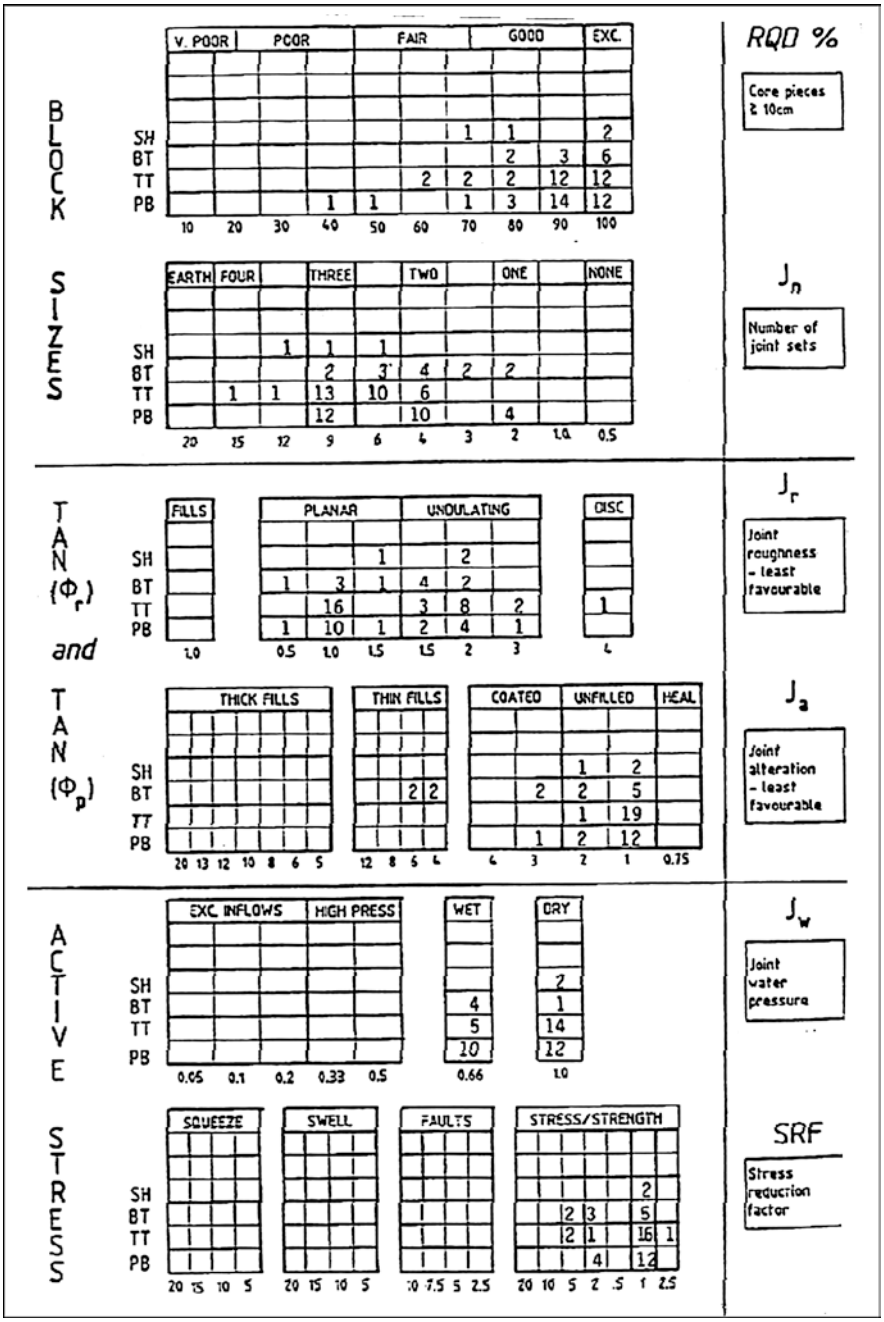

Fig. 18.6 Integrated rock mass classification data base from cliff mapping, precedent tunnel mapping and core logging, which could have been used for predicting expected conditions in the Channel Tunnel

Table 18.1 Synthesis of the pre-construction sources of rock quality for the chalk marl

Parameter	(mean)	Description	Sum/number of observations	Typical range
RQD	90.1	Excellent	6940/77	90–100
J_n	6.5	Two joint sets plus random	473/73	4–9
J_r	1.5	Rough, planar joints	93/63	1–2
J_a	1.5	Slight alteration	79/53	1–2
J_w	0.9	Slight water inflow	42/48	0.66–1.0
SRF	1.5	Slight stress problems	74/48	1–2

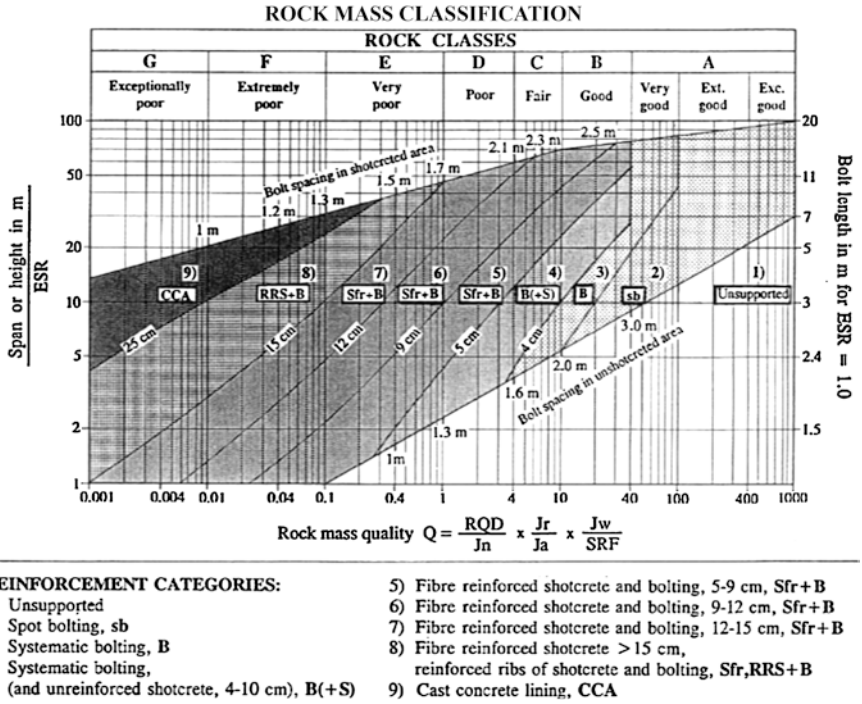

Fig. 18.7 *Q*-support diagram showing the required spans for unsupported openings (lower diagonal line) and support measures when this span is exceeded (Grimstad and Barton 1993)

original circular cross-section after 100 years is reasonable. The worst regions of overbreak and failure presumably have *Q*-values of between about 0.2 (Beaumont minimum) and 1.0. The "no support required" lower diagonal line in Fig. 18.7 is slightly conservative (compared to mining practice) since it reflects civil engineering practice. (This diagonal line is unchanged since 1974, when the *Q*-system was first published.)

18.6 The Possibility of Overbreak Problems in the Channel Tunnels

The mean value of $Q = 8$ for the whole sample of Chalk Marl (as characterised by the first author prior to MST and MRT assessment) and the foregoing analysis of frequency of occurrence, leads to the following possible scenario for evaluating the potential for overbreak in poorer ground. We will assume the occurrence of the following (frequently observed) local conditions and their cumulative effect on the mean *Q*-value:

1. Three joint sets ($J_n = 9$)
2. Smooth, planar joints ($J_r = 1.0$)
3. Slightly altered joint walls ($J_a = 2.0$)
4. Medium water inflow (>5 L/min locally) ($J_w = 0.66$)

The successive, cumulative effects that these frequently observed conditions will have, compared to the weighted mean *Q*-value of 8.0, are as follows:

$$Q = 8.0 \rightarrow 5.8 \rightarrow 3.9 \rightarrow 2.9 \rightarrow 1.9$$

This progressive worsening moves both MST and MRT size tunnels well into the regions of the *Q*-support diagram that require support close to the tunnel face. The majority of the original *Q*-system case records were, however, related to drill-and-blast tunnels and caverns. During the instant of excavation, blocks of rock that are inherently unstable due to unfavourable J_n, J_r and J_a values (perhaps combined with "external" factors like stress and water pressure) will tend to fall out in the excavation process and contribute to overbreak.

When equally unstable blocks are freed by a TBM cutter head, many of them will try to fall out on the shield or trailing fingers. However, a good percentage of them will probably remain in place since they were not disturbed as much by the TBM as by blasting which involves blast gas penetration and higher levels of vibration. The lower frequency of vibration in a TBM excavation scenario may well lead to less overbreak, but overbreak that does occur is of course more problematic when trying to build pre-cast linings. The fact that the MST tunnel is "left unsupported" for 3.5 diameters (17 m to first ring) and that the larger MRT tunnel is "left unsupported" for 2.0 diameters (18 m to first ring) means that overbreak problems are likely when local conditions follow the worsening and likely scenarios outlined above.

The MST and MRT have diameters approximately two to four times that of the Beaumont Tunnel. They are not subjected to such high rock stresses as at the undercliff part of Beaumont, but they are in many locations subjected to several more serious factors such as more adverse joint orientations, weathering effects and high pore pressures in the sub-vertical joints connected to the sea bed. The increased tunnel sizes induce a fundamental scale effect, where unchanged joint frequency causes greater problems with overbreak, the larger the tunnel diameter. In the *Q*-system, this scale effect is reflected in a greater need for immediate temporary support and final support, the larger the tunnel.

The need for a certain level of support in the case of large tunnels even with "good" rock quality ($Q > 10$) is demonstrated in Fig. 18.7.

18.7 Preliminary Review of TML *Q*-logging in the MST AND MRT

TML made extensive use of the *Q*-system in describing (under difficult mapping conditions) the rock mass conditions encountered. In the Marine Service Tunnel (MST), approximately 250 face logs and approximately 1120 sidewall logs between chainage km 20 and 30, provide a wealth of information on TML's *Q*-system estimates, which, taken together with their careful descriptions of tunnelling conditions and joint characteristics, give a very useful data base from which to draw conclusions on the encountered conditions.

The conditions under which TML's observations were obviously made were not ideal, due to limited access to the rock, as is typical with TBM. However, numerous and more extensive mapping results were available from cross-passages to supplement the necessarily sparser data sets from the face and sidewall logs. These were carefully reviewed, and an assessment made of the validity of TML's estimates.

Output from TML computer file print-out provided by Eurotunnel were analysed in four different ways as follows:

1. distributions of *Q* for km 20–30
2. distributions of *Q* for km 20–24
3. distributions of *Q* for km 24–30
4. distributions of *Q* for km 20.5–21.3

In the first stage of analysis that follows, both face logs and side wall logs were analysed. Due to the presence of swarf, the latter may be a less reliable source of data, and side wall logs are subsequently excluded from our analysis in Sect. 18.8.

TML's average estimate of *Q* for these 10 km in the MST was 22.9 (good), though most frequent observations were in the "very good" class (*Q* = 40–100). Comparison of TML estimates for km 20–24 and km 24–30 in the MST reflect both the poorer quality of rock in the early sub-sea kilometres, and the more accurate description of conditions that was possible when overbreak due to jointing was frequent. Average *Q*-values were 9.9 (fair) and 33.4 (good) respectively. The most frequent rock class observed in km 20–24 was "fair" (*Q* = 4–10, mean 6.3, 270 observations). The most frequent rock class observed in km 24–30 was "very good" (*Q* = 40–100, mean = 50, from 380 observations).

Table 18.2 shows the range of TML's observations in the MST for the poorer ground between km 20 and 24, and Table 18.3 shows the range of TML's observations in the MST for the low-cover and *poorest ground* between km 20.5 and 21.3.

TML's *Q*-system classification of the low cover zone (km 20.5–21.3) in the MST (Table 18.3) gave a mean *Q* = 5.6 (fair) with most frequent observations in the "fair" (*Q* = 4–10) and "poor" (*Q* = 1–4) classes.

Maximum ranges and mean values of *Q* estimated by TML for the various zones mapped in the MST between 20 and 30 km fairly closely resemble the first author's independently derived predicted conditions obtained from core logging (PB series)

Table 18.2 TML's *Q* estimates for km 20–24, from face and side-wall logging in the MST (marine service tunnel)

Range of *Q*	Description	No. of observations	Sum of actual *Q*-values	Mean *Q*-values
0.1–1	Very poor	5	3.2	0.6
1–4	Poor	191	470.4	2.5
4–10	Fair	272	1708.7	6.3
10–40	Good	96	1577.4	16.0
40–100	Very good	47	2280.0	49.0
	Totals	611	6039.7	9.9 (fair)

Table 18.3 TML's *Q* estimates for the worst-quality chainage km 20.5–21.3, from face and side-wall logging in the MST (marine service tunnel)

Range of *Q*	Description	No. of observations	Sum of actual *Q*-values	Mean *Q*-values
0.1–1	Very poor	2	1.5	0.7
1–4	Poor	42	90.6	2.2
4–10	Fair	45	275.9	6.1
10–40	Good	14	213.1	15.0
40–100	Very good	0	0.0	0.0
	Totals	103	581.1	5.6 (fair)

and precedent experience (Beaumont and Terlingham Tunnels). The following list compares the two sets of data:

TML mapping during construction of the MST:		
km 20–30	*Q* (range) = 0.3–100	*Q* (mean) = 22.9
km 20–24	*Q* (range) = 0.3–40	*Q* (mean) = 9.9
km 20.5–21.3	*Q* (range) = 0.7–20	*Q* (mean) = 5.6
Author's estimates from pre-construction sources:		
PB1 to PB8	*Q* (range) = 1.5–50	*Q* (mean) = 12.6
Terlingham Tunnel	*Q* (range) = 1.3–50	*Q* (mean) = 10.6
Beaumont Tunnel	*Q* (range) = 0.2–100	*Q* (mean) = 3.4

Comprehensive data packages were analysed by the first author at ten well documented chainages within km 20–30, in order to independently check TML's methods of *Q*-system application in the various qualities of rock. Some rather small but consistent errors in their application of the *Q*-system included a non-conservative use of $J_w = 1.0$ in many cases where significant water flow was observed and where $J_w = 0.66$ should have been used. In contrast, TML consistently used a conservative value of SRF = 2.5 in all cases, while only a limited number of the poorer, low cover tunnel sections perhaps qualify for this "low stress, near surface" characterisation.

In the poorest qualities of rock where TML's structural descriptions were quite comprehensive and accurate due to joint delineated overbreak, TML's estimates of *Q* were very similar to those of the author. At the ten well-documented sections

Table 18.4 Comparison of TML and the first author's *Q*-estimates at well documented MST and MRT chainage between km 19.8 and 27.2

	Author's estimates of *Q*		TML estimates of *Q*	
Chainage (± 50 m)	*Q* (range)	*Q* (mean)	*Q* (range)	*Q* (mean)
1. 19,824 km	7.5–50	17.6	2.4–80	28.9
2. 19,925 km	0.9–25	7.5	1.7–40	11.4
3. 20,651 km	1.0–100	7.8	1.6–40	11.7
4. 21,026 km	1.7–50	9.4	4.4–13.2	7.4
5. 22,151 km	1.2–17	5.7	2.4–19	7.0
6. 22,526 km	1.2–17	5.6	3.0–6.7	4.9
7. 22,901 km	0.5–20	2.6	1.8–10.7	4.9
8. 23,276 km	0.5–25	3.7	1.1–8.2	4.0
9. 23,651 km	1.5–25	5.7	2.5–13.3	7.9
10. 27,025/167 km	9.9–133	12.4	3.0–80	16.2

between km 20 and 30, careful interpretation was made of TML's face and tailskin logs for the MST, and of their logs of cross-passages and vertical and sideways probes. The following results were obtained:

TML: range of mean $Q = 4.0–28.9$, overall mean $Q = 10.4$
Author: range of mean $Q = 2.6–17.6$, overall mean $Q = 7.8$

Details of this comparison are given in Table 18.4.

In these well documented cases, an example of which is shown in Fig. 18.8, there is no question about the poor quality of the ground, and the first author's estimates are in fact slightly more conservative than TML's estimates. Conditions encountered were well within the range predictable from pre-construction information if the necessary classifications (of pre-construction sources of information) had been performed.

18.8 Detailed Review of TML Face Logging Results

In the foregoing section TML's *Q*-logging was analysed, using both the TBM face logs and the TBM side wall logs. As indicated earlier, the latter might be expected to be affected by the swarf. In this section we have therefore included only the results of TML's face logging. This is a significantly smaller data base as can be seen when comparing with the numbers in parentheses (from Tables 18.2 and 18.3) (Table 18.5).

A similar comparison between face logging results and the full data set (from Table 18.3) is given for the low cover section (km 20.5–21.3) in Table 18.6.

If we again analyse just the face logging results, but include both the MST and both the MRT (marine running tunnels, of 8 m diameter), we obtain the results given in Tables 18.7 and 18.8 for the chainage km 20–24, and for the poorest quality, low-cover section km 20.5–21.3.

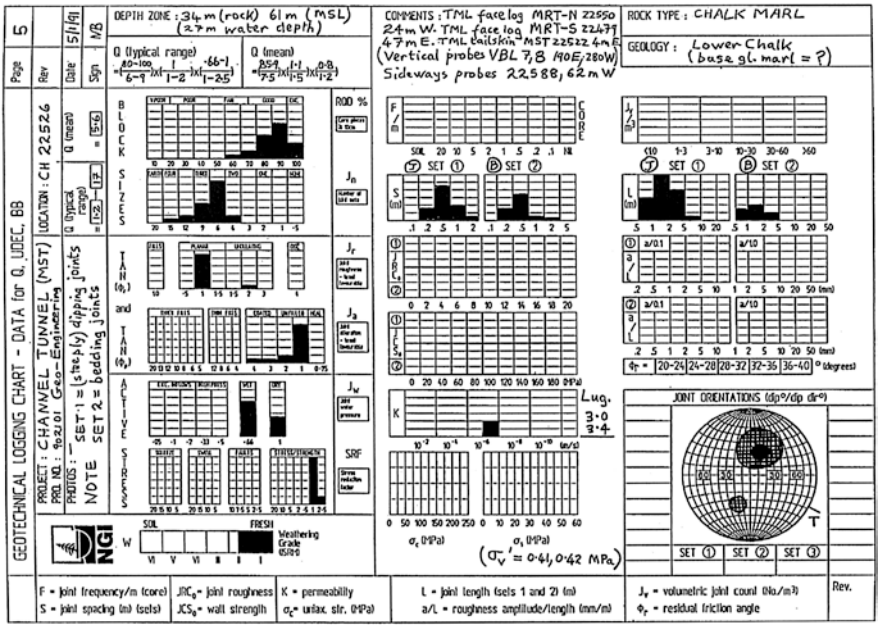

Fig. 18.8 Example of *Q* and Geotechnical log at well documented section for MRT/MST at ch. 22.526 m. Note that the most frequent ratio of J_n/J_r is 6/1, but 9/1 is also frequent. Refer to Fig. 18.9 example linking overbreak to J_n/J_r

Fig. 18.9 An example of the overbreak experienced in the chalk marl, as observed here in one of the piston relief ducts (PD39) between the running tunnels. Two smooth near-vertical joint sets are seen. This is a classic example of $J_n/J_r = 9/1.0$, symbolising the likelihood of overbreak, since $J_n/J_r \geq 6$, according to subsequent conclusions in Barton (2007)

Table 18.5 TML's MST face logging results, km 20–24

Range of *Q*	Description	No. of observations	Mean *Q*-values
0.1–1	Very poor	0 (5)	– (0.6)
1–4	Poor	18 (191)	2.2 (2.5)
4–10	Fair	17 (272)	6.0 (6.3)
10–40	Good	9 (96)	14.6 (16.0)
40–100	Very good	5 (47)	40.0 (49.0)
	Totals	49 (611)	9.7 (9.9)

The numbers in parentheses are from Table 18.2

Table 18.6 TML's MST face logging results, km 20.5–21.3. (The numbers in parenthesis are from Table 18.3)

Range of *Q*	Description	No. of observations	Mean *Q*-values
0.1–1	Very poor	0 (2)	– (0.7)
1–4	Poor	8 (42)	2.0 (2.2)
4–10	Fair	6 (45)	6.2 (6.1)
10–40	Good	3 (14)	11.7 (15.0)
40–100	Very good	0 (0)	– (–)
	Totals	17 (103)	5.2 (5.6)

Table 18.7 TML's face logging of all marine tunnels, km. 20–24

Range of *Q*	Description	No. of observations	Mean *Q*-values
0.1–1	Very	0	–
1–4	Poor	51	2.8
4–10	Fair	52	6.2
10–40	Good	24	15.5
40–100	Very good	10	40.0
	Totals	137	9.0

Table 18.8 TML's face logging of all marine tunnels, low-cover section, km 20.5–21.3

Range of *Q*	Description	No. of observations	Mean *Q*-values
0.1–1	Very poor	0	–
1–4	Poor	13	2.3
4–10	Fair	22	6.0
10–40	Good	12	13.4
40–100	Very good	5	40.0
	Totals	50	10.5

Summarising the above analyses of potential differences between face logs and side wall logs, we can observe that TML's average estimate of *Q* for km 20–30 was 22.9 for all logs, but only 10.3 considering solely the face logs within the Chalk Marl. For MST (marine service tunnel) km *20–24*, TML's average *Q*-values were 9.9 (for all logs) and 9.7 (for face logs). In this case the difference is rather small, as

also seen in Table 18.5. For MST km *24–30*, TML's average *Q*-values were 33.4 (for all logs) but only 17.3 (for face logs). In fact apart from the low-cover section in particular, and ch. 20–24 in general, the good quality chalk marl experienced in *most* of the tunnel did indeed prove ideal for TBM tunnelling, and the world records for this tunnel, in the 8–9 m diameter class, attributed to Robbins TBM, remain to this day (best day 75 m, best week 428 m, best month 1719 m, best monthly average 873 m). For further details of the TBM performances see Warren et al. (1992), Table 14.2.

The most frequent rock class observed for MST km 20–24 was "fair" (all 272 logs, mean $Q = 6.3$), and "poor" to "fair" (35 face logs, mean $Q = 4.1$). The most frequent rock class observed for MST km 24–30 was "very good" (all 380 logs, mean $Q = 50$), and "fair" to "good" (30 face logs, mean $Q = 11.7$), in this case a marked reduction. *It is therefore seen that the face log interpretation generally gave a somewhat lower value of Q than the combined face and side wall logs.* This is to be expected due to the problem of swarf smearing over joint traces, making observations very difficult or impossible.

An important point to be noted in the above analyses is that the MST entered Glauconitic Marl and then Gault/6A material between chainage km 26.2 and 29.1 as it deviated to the north and below the level of the adjacent running tunnels past the UK Crossover cavern. Ideally this section of MST values should be ignored if considering solely Chalk Marl (Fig. 18.9).

The poor conditions encountered between km 20 and 24, and in particular from the low cover section between km 20.5 and 21.3 indicate mean *Q*-values logged by TML that are virtually identical to the weighted mean value $Q = 8$ obtained from the precedent experience described earlier (PB1 to PB8 drill core, Terlingham and Beaumont tunnels).

18.9 Use of Precedent Data in Predicting Tunnelling Problems

In Fig. 18.6 the *Q*-system histograms for the combined observations of ***Terlingham and Beaumont Tunnels, of the PB series core and of Shakespeare Cliffs and foreshore***, gave the following "most frequent" and "next most frequent" occurrences:

1. Most frequent $Q = 100/9 \times 1/1 \times 1/1 = 11.1$
2. Next most frequent $Q = 90/4 \times 2/2 \times 0.66/2 = 7.4$

From these two theoretical cases, it was reasonable to surmise that higher water inflows and slight joint alteration were more likely to be present with three joint sets ($J_n = 9$) than with two joint sets. A third class was therefore predicted as follows:

3. **Possible problem ground $Q = 90/9 \times 1/2 \times 0.66/1 = 3.3$**

Each of these six parameter values were frequently observed (i.e. most frequently or next most frequently) and they combine to form a logical physical reality. If an

SRF value of 2.5 had been used (the shallow siting assumption made by TML), an even poorer quality (Q = 1.7) could have been reasonably predicted.

The same procedure of histogram analysis will now be followed for ***seven detailed structural data packages within the chainage km 20–24.*** The most frequently and next most frequently estimated Q parameters for the seven relevant data packages within this chainage were as follows:

1. Most frequent $Q = 90/5.8 \times 1/1 \times 0.9/1 = 13.2$
2. Next most frequent $Q = 88/6.6 \times 1.4/2.5 \times 0.8/2.3 = 2.6$

If we proceed as before and combine the most frequently and next most frequently observed parameters in the generally *least favourable* manner, we arrive at the third category:

3. **Possible problem ground $Q = 88/6.6 \times 1.0/2.5 \times 0.8/1.0 = 4.3$**

If TML's SRF value of 2.5 had been used as before, an even poorer quality (Q = 1.8) is obtained. This range of problem ground (Q = 1.8–4.3) is remarkably similar to that deduced earlier from pre-construction data (Q = 1.7–3.3) and suggests that poor ground conditions were predictable.

It is worth noting that users of a rock mass classification systems such as the Q-system (and RMR) will be on the lookout for joints and unfavourable features (in outcrops, tunnels and drill core) and may arrive at an overly pessimistic classification of the ground even when less jointed conditions are represented in their logging. The above analysis and comparison of pre-construction *predictable* conditions and post-construction *observable* conditions may therefore be a little unfair, if it turns out that one is comparing the generally poorer zones observed in the Terlingham and Beaumont Tunnels and in the PB core, with more average conditions in the chainage interval km 20–24.

The five worst sections logged by TML received the lowest Q-values according to TML logging (refer to Table 18.4). The first author's mean Q-estimates at the same chainages, based on the extensive documentation given by TML are given on the right hand side of TML's estimates in Table 18.9.

A set of Q-system histograms for one of these five chainages was given in Fig. 18.8. An analysis of the frequency of Q-parameter observations for these five sections is given in Fig. 18.10. From this we can derive data for the three categories "Most frequent", "next most frequent" and "possible problem ground" as before. The following results are obtained:

1. Most frequent $Q = 90/6 \times 1/1 \times 0.66/1 = 10.0$
2. Next most frequent $Q = 100/9 \times 2/3 \times 1/2.5 = 3.0$

Table 18.9 Comparison of TML's and the first author's estimates of mean Q-values at five well-documented sections in poorer ground

Chainage	TML	Author
km 21.026 =	7.4	9.4
km 22.151 =	7.0	5.7
km 22.526 =	4.9	5.6
km 22.901 =	4.9	2.6
km 23.276 =	4.0	3.7

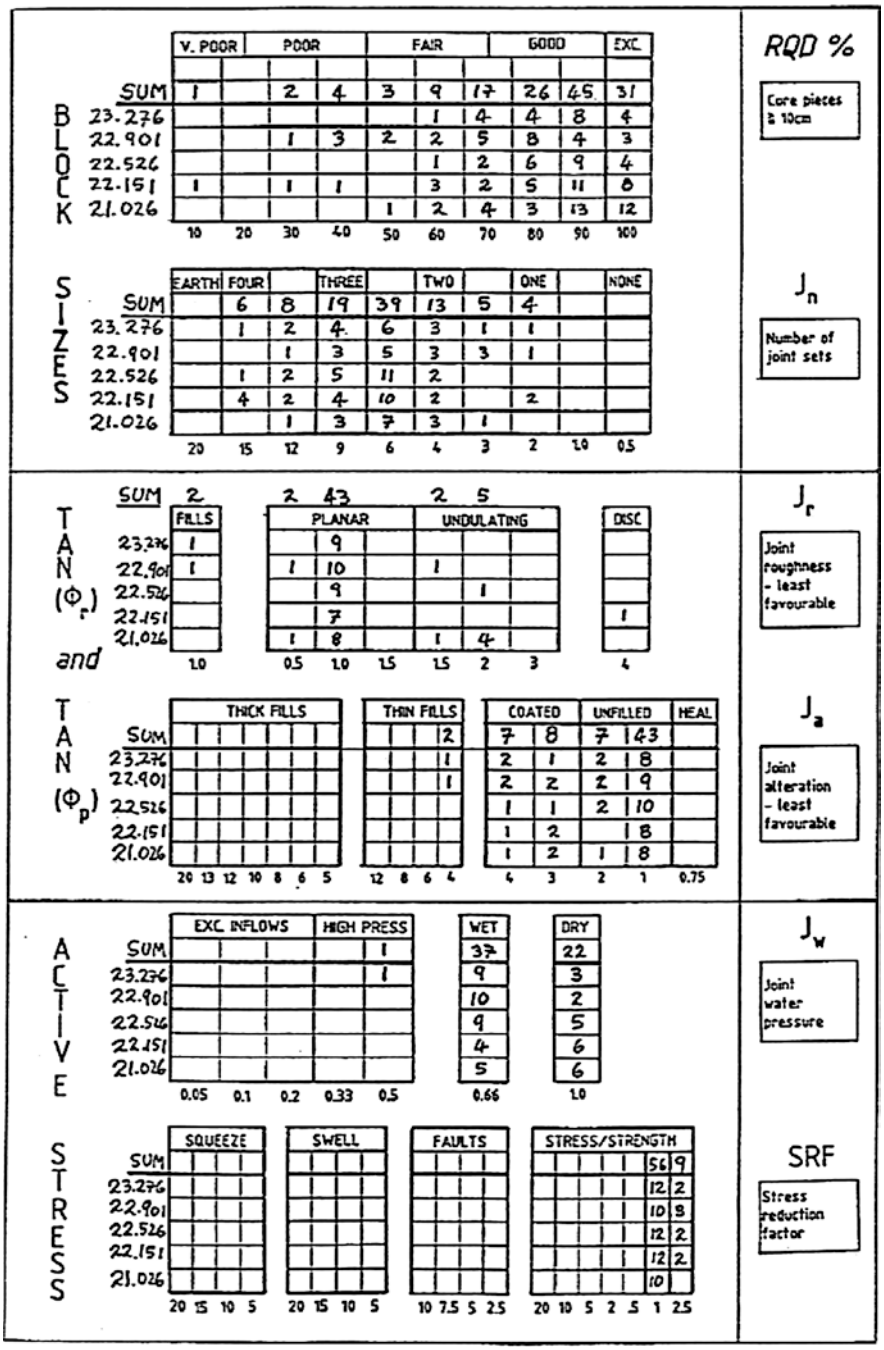

Fig. 18.10 Analysis of five of the poorest Channel Tunnel chainages in sub-sea, permeable, and partially weathered sections

If we proceed as before and combine the most frequently and next most frequently observed parameters in the generally least favourable manner, we arrive at the third category:

3. **Possible problem ground $Q = 90/9 \times 1/3 \times 0.66/1 = 2.2$**

If the above minimum value of SRF = 2.5 had also been used as before, an even poorer quality ($Q = 0.9$) is obtained. Table 18.10 finally compares the predictable conditions with those in the 20–24 km sections, using the "most frequently" observed, the "next most frequently" observed and the "possible problem ground" categories described above.

In view of the fact that the Q-value is based on a rating and calculation method ($a/b \times c/d \times e/f$) that results in a "logarithmic-like" scale (minimum 0.001, maximum 1000), the closeness of the predicted and observed conditions is emphasised. With rock masses of relatively poor quality, the "possible problem ground" ($Q = 0.9$–4.3) will inevitably have caused overbreak when excavated by TBM, and especially when 17–18 m of tunnel length is without support until the PC-element assembly is reached (and the liner is suitably stiffened with pea-gravel and grouting). The marine running tunnels are of sufficient diameter (8.4 m) that the "next most frequent" Q range of 2.6–7.4 will also undoubtedly have led to overbreak, and specific problems for the contractor when (unfortunately) wedge-lock and not bolted PC-elements were designed for the UK side of the project.

A glance at Fig. 18.7 indicates the level of NMT style permanent support (Barton and Grimstad 1994) actually required in support classes 4 and 5 when Q-values are less than 10. For the case of a drill-and- lasted or road-header excavated tunnel, the necessary support would be systematic bolting and shotcrete, with steel fibre reinforcement in the poorest classes of rock. If stresses were higher, and the SRF factor became

Table 18.10 Comparison of predictable and encountered conditions based on Q-values calculated from the most frequent observed conditions, followed by next most frequent, and finally possible problem ground

Data from	Most frequent	Next most frequent	Possible problem ground
Predicted conditions (Pre-construction data)	$Q = 11.1$ $\left(\frac{100}{9}\right)\times\left(\frac{1}{1}\right)\times\left(\frac{1}{1}\right)$	$Q = 7.4$ $\left(\frac{90}{4}\right)\times\left(\frac{2}{2}\right)\times\left(\frac{0.66}{2}\right)$	$Q = 1.7$–3.3 $\left(\frac{90}{9}\right)\times\left(\frac{1}{2}\right)\times\left(\frac{0.66}{1-2}\right)$
Encountered conditions (typical: km 20–24)	$Q = 13.2$ $\left(\frac{90}{5.8}\right)\times\left(\frac{1}{1}\right)\times\left(\frac{0.9}{1}\right)$	$Q = 2.6$ $\left(\frac{88}{6.6}\right)\times\left(\frac{1.4}{2.5}\right)\times\left(\frac{0.8}{2.3}\right)$	$Q = 1.8$–4.3 $\left(\frac{88}{6.6}\right)\times\left(\frac{1}{2.5}\right)\times\left(\frac{0.8}{1-2.3}\right)$
Encountered conditions (Poorest: km 20–24)	$Q = 10.0$ $\left(\frac{90}{6}\right)\times\left(\frac{1}{2}\right)\times\left(\frac{.66}{1}\right)$	$Q = 3.0$ $\left(\frac{100}{9}\right)\times\left(\frac{2}{3}\right)\times\left(\frac{1}{2.5}\right)$	$Q = 0.9$–2.2 $\left(\frac{90}{9}\right)\times\left(\frac{1}{3}\right)\times\left(\frac{0.66}{1-2.5}\right)$

"mobilised" by unfavourable ratios of principal stress to uniaxial compression strength, then heavier support would of course be needed. A drained lining and satisfactory drainage measures are of course a prerequisite for this NMT style of support.

18.10 Utilisation of Seismic Measurements

Offshore geophysics carried out during several campaigns in preparation for the Channel Tunnels indicated P-wave velocities generally in the region of 2.0–2.6 km/s for the UK Chalk Marl. These low values reflect the low compressive strength and the relatively high porosity of the Chalk Marl. Extensive laboratory testing of the Unit 2 Chalk Marl through which most of the UK tunnels were driven showed the average values assembled in Table 18.11.

During the years since the Channel tunnel was completed, developments have been made in linking seismic velocity measurements with *Q*-value descriptions of rock mass quality (Barton 1995, 2002, 2006). The objective has been to improve tunnel support prognoses based on refraction seismic measurements. This work was accelerated by direct calibration of core logging results with adjacent cross-hole seismic tomography. An initial calibration between Q and V_p was obtained for shallow, jointed, hard rock sites for which the following proved to be a quite accurate method (Barton et al. 1992a, b).

$$V_p = 3.5 + \log_{10} Q \tag{18.2}$$

Subsequently, seismic measurements and rock quality assessments from many sites around the world, including chalks, sandstones and other weak rocks, were added to the data base, providing the opportunity to extend the correlation to weak porous rocks at variable depth.

Figure 18.11 shows the most recent version of these correlations. The central (thick) diagonal line gives the relationship between V_p and Q shown in Eq. (18.2), for which $Q_c = Q$ (when uniaxial strength σ_c approximates 100 MPa) The "normalising" of the Q-value by direct application of the uniaxial strength is a necessary

Table 18.11 Laboratory index test values for Unit 2 Chalk Marl

		Average	Min/Max
Uniaxial compressive strength	MPa	5.9 (252)	0.6/17.8
Young's modulus (vertical)	GPa	0.64 (37)	0.15/4.2
V_p (axial)	km/s	2.44 (152)	1.26/3.27
V_p (transverse)	km/s	2.62 (144)	1.37/3.58
Specific gravity	g/cm^3	2.71 (72)	2.67/2.73
Dry unit weight	g/cm^3	1.96 (289)	1.63/2.30
Moisture content	%	13.3 (288)	5.8/23.8
Porosity (calculated)	%	27.7 –	15.7/39.0

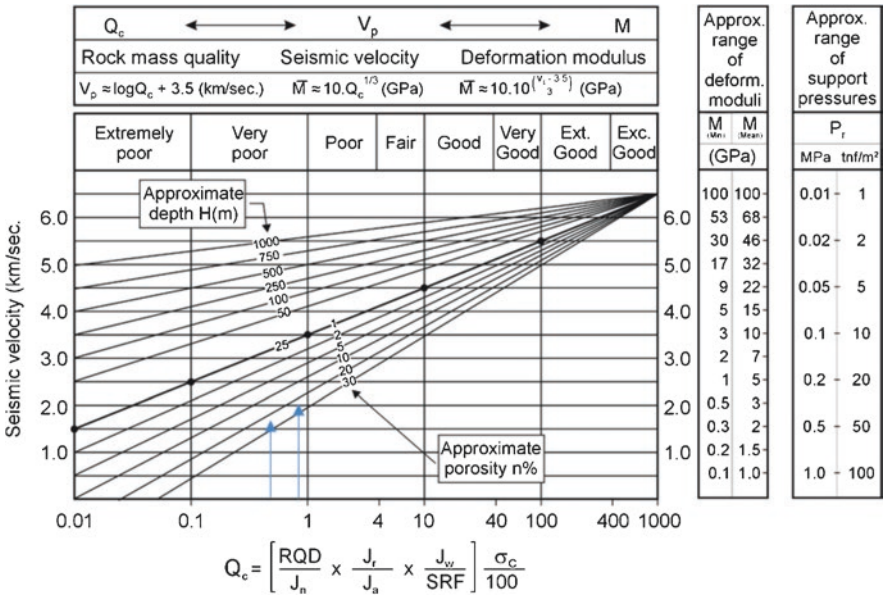

Fig. 18.11 Seismic correlations chart for interrelating Q, V_P, M and depth (with negative correction for porosity which is approximate) (Barton 1995). The higher velocities at depth were empirical results resulting from deep cross-hole seismic velocity measurements (at the UK Nirex site), and Q-logging of 11 km of boreholes by NGI/Atkins colleagues (Barton et al. 1992b)

modification for very weak (and very strong) rocks, and further correction is provided by the porosity and depth.

In order to illustrate the use of this seismic correlation chart, we can take the weighted mean value of Q = 8 from our precedent study (PB1 to PB8 core, Terlingham and Beaumont tunnels). This value is very close to the TML mean of Q = 9 for km 20–24 obtained from all the face logs in the MST, MRTN and MRTS. (Refer back to Table 18.7.)

Since Q (mean) = 8, and σ_c (mean) = 6 MPa, therefore Q_c (mean) = 8 × (6/100) = 0.5

This Q_c value intersects the reference diagonal line (Eq. 18.2) at V_p = 3.2 km/s. Correction for average porosity (n = 27.7%, Table 18.11) results in a reduction of 1.6 km/s giving 1.6 km/s. However, tunnel depths of, for example, 40 m (see Fig. 18.12) brings this value up to about 2.0 or 2.1 km/s. Even lower values appear likely in the shallow cover (20 m) zone between km 20.5 and 21.3.

In those sections of the tunnel with markedly higher Q-values, that is, Q = 15 (approximately) for the MST between km 24 and 30 (excluding 26.2–29.1) we have the following:

Q (mean) = 15, σ_c (mean) = 6 MPa, therefore Q_c (mean) = 15 × (6/100) = 0.9

This Q_c-value intersects the reference diagonal line (Eq. 18.2) at V_p = 3.4 km/s. Correction for average porosity (n = 27.7%) results in a reduction of 1.4 km/s, giv-

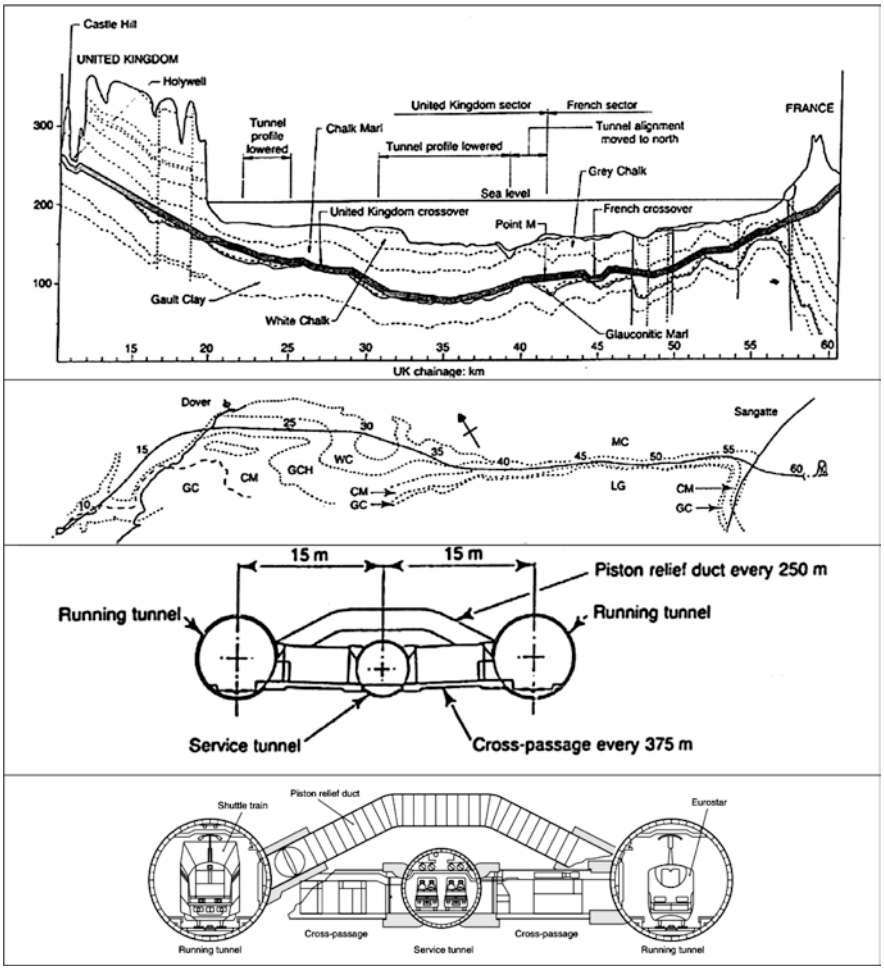

Fig. 18.12 Top: Channel tunnel stratigraphy, indicating that the tunnels mostly followed the chalk marl on the English side. The low-cover section from ch. 20–24 starts from close to the Shakespeare Cliffs. Note also the location of the UK cross-over cavern (Fugeman et al. 1992; Varley et al. 1992). Water depths are shown in the second diagram. The third diagram shows relative dimensions of the MST (5.3 m dia.) and MRT (8.4 m dia.) tunnels, and the cross-passages and smaller piston relief ducts. The final diagram is from Japan Railway and Transport Review 26, 2001, and shows the Eurostar London-to-Paris trains

ing 2.0 km/s. Tunnel depths of up to 40 m (approx.) bring this value up to about 2.5 km/s. An uncertainty in the above correlations which potentially show excellent agreement with the offshore geophysics (typically 2.0–2.6 km/s) is the effect of water depth and effective stress. Where permeability is very low due to less interconnected structure, the water could perhaps be considered as an additional load thereby potentially increasing the velocity and modulus of deformation. In permeable sections with a lot of structure, the water pressure giving significantly reduced

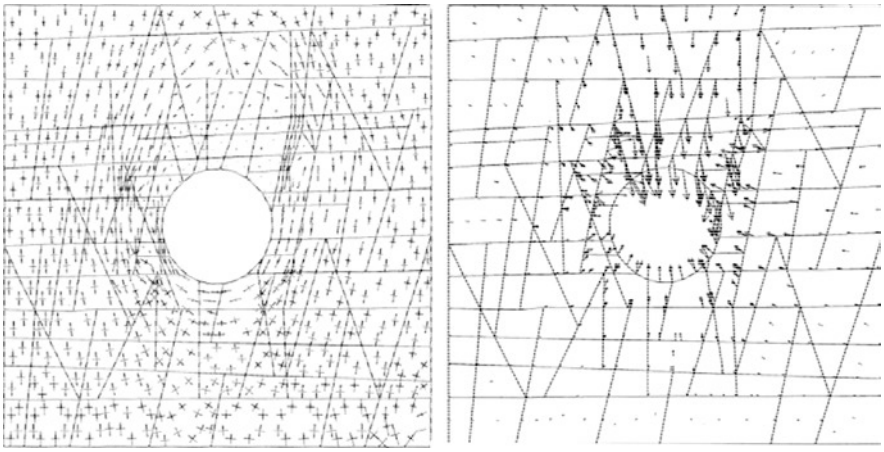

Fig. 18.13 Low effective stresses (left), particularly in the horizontal direction, combined with the low JRC estimates (see logging data in Fig. 18.3), meant that predicted vertical deformation (right), and maximum joint shearing could be several millimetres. A 50 m deep simulation of the 5.3 m diameter MST. UDEC-BB model, pers. comm. Makurat 1990)

effective stress would presumably have resulted in velocities of between 1.5 and 2.0 km/s according to the trends exhibited in Fig. 18.11. Due to the changed tunnel location in relation to earlier offshore boreholes and seismic lines, it is not clear whether these potentially lower and adverse velocity values were registered.

The third parameter illustrated in Fig. 18.11—deformation modulus *M*—is subject to considerable uncertainty due to effective stress effects, and disturbance effects when measured in situ, and due to the EDZ or excavation disturbed zone effect of reduced modulus immediately surrounding the tunnel in a rock mass with *apparently unchanged* characterisation. An undisturbed, fully *confined* modulus prediction of 3–5 GPa (*M* mean) and a fully *disturbed* modulus prediction of 0.5–1 GPa (Fig. 18.11) may well be in line with the assumed near-tunnel values of about 0.8–1.4 GPa that were derived by back-analysis of TBM tunnel deformation measurements by Eves and Curtis (1992).

For reference purposes the location of the tunnel in the geology of the English Channel is illustrated in Fig. 18.12, together with water depths and the relative dimensions and separation (15 m c/c) of the TBM tunnels. The combination of shallow tunnels, a permeable rock mass (in the low-cover section) and a significant water depth, and also the relatively low density rock (Table 18.11), meant that effective stresses could be rather low, and represent a challenge for not only overbreak, but also stability, as indeed shown in the contemporary (1990) distinct element modelling (UDEC-BB) performed by Makurat (Priv. Comm.) which is reproduced in Fig. 18.13.

18.11 Conclusions

In a drill and blasted tunnel, overbreak occurs as part of the excavation cycle and support can be applied right to the face, something which was not feasible with the chosen TBM method. Unsupported tunnel lengths of 17 and 18 m for the MST and MRT service and running tunnels represent approximately 3.5 and 2 diameters of unsupported rock in a rock mass with an average predicted rock mass quality *Q* of about 8, but with a quality range of at least 1–50. Tunnels of 8.4 m and 5.3 m span require rock mass qualities of 40 and 10 (respectively) for no support to be required according to case record analysis in the *Q*-system. Since rock mass quality between 20 and 24 km in the low-cover section was generally below 10 and much below 40, problems with stability (overbreak) were predictable and inevitable. Sensitivity studies using the most frequently observed *Q*-system parameters indicate that combinations of three joint sets, smooth joints, high water pressure, locally weathered joints, would inevitably lead to overbreak and the need for immediate support if it should be avoided. Overbreak with blocks falling onto the trailing fingers was therefore inevitable in many locations in this sub-sea chainage. In general, remarkable consistency was shown between the "blind logging" of precedent sources of data for the chalk marl (Terlingham and Beaumont tunnels, PB-series sub-sea cores), and the extensive logging in the three TBM drives by the contractor TML. The latter data sets were subsequently provided for comparison in this paper. It is interesting to also note the closeness of the TML *Q*-logging in the UK cross-over cavern ($Q = 2.5$–13, mean $Q = 7$) to precedent sources of *Q* (Birch and Rankin 1992). These *Q*-values are in the poor to fair category and proved to be a challenge for this important NATM cavern at one particular location, where vertical deformations increased suddenly from 30 to 90 mm in March 1990 (Varley and Warren 1995). Recently developed correlations between seismic velocity and *Q*-value using porosity, depth and uniaxial compressive strength appear to be promising ways of improving prognoses of rock quality and tunnelling problems in future projects.

Acknowledgements The work described in this chapter was performed for Geo-Engineering who were under contract for Eurotunnel. The permission of Eurotunnel and of Dr John Sharp of Geo-Engineering to publish this comprehensive analysis is gratefully acknowledged.

References

Barton N (1993) Physical and discrete element models of excavation and failure in jointed rock. Keynote lecture. ISRM Int. Symp. on Assessment and Prevention of Failure Phenomena in Rock Engineering, Istanbul, Turkey

Barton N (1995) The influence of joint properties in modelling jointed rock masses. Keynote lecture. 8th ISRM Congress, Tokyo, vol 3. Balkema, Rotterdam, pp 1023–1032

Barton N (2002) Some new Q-value correlations to assist in site characterization and tunnel design. Int J Rock Mech Min Sci 39(2):185–216

Barton N (2006) Rock quality, seismic velocity, attenuation and anisotropy. Taylor & Francis, Abingdon, p 729

Barton N (2007) Future directions for rock mass classification and characterization – towards a cross-disciplinary approach. Invited lecture. Proc. of 1st US-Canada Rock Mech. Symp., Vancouver, pp 179–188

Barton N, Choubey V (1977) The shear strength of rock joints in theory and practice. In: Rock mechanics, vol 1/2. Springer, Vienna, pp 1–54

Barton N, Grimstad E (1994) Rock mass conditions dictate choice between NMT and NATM. Tunnels & Tunnelling, October 1994, pp 39–42

Barton N, Shen B (2017) Extension failure mechanisms explain failure initiation in deep tunnels *and* critical heights of cliff faces and near-vertical mountain walls. US Rock Mech. Symp. San Fransisco, ARMA17-686, 20p

Barton N, Lien R, Lunde J (1974) Engineering classification of rock masses for the design of tunnel support. Rock Mech 6(4):189–236

Barton N, Grimstad E, Aas G, Opsahl OA, Bakken A, Pedersen L, Johansen ED (1992a) Norwegian method of tunnelling. WT focus on Norway. World tunnelling. June/August 1992

Barton N, Loset F, Smallwood A, Vik G, Rawlings C, Chryssanthakis P, Hansteen H, Ireland T (1992b) Geotechnical core characterization for the UK radioactive waste repository design. Proc. of ISRM Symp. EUROCK, Chester, UK

Birch GP, Rankin WJ (1992) Geotechnical aspects of the UK undersee Crossover. Ch. 22. Proceedings of the Institution of Civil Engineers. The Channel Tunnel

Cundall P (1980) A generalized distinct element program for modelling jointed rock. Report PCAR-1-80. Contract DAJA37-79-C-0548, European Research Office, US Army. Peter Cundall Associates

Eves RCW, Curtis DJ (1992) Tunnel lining design and procurement. Proceedings of the Institution of Civil Engineers. The Channel Tunnel. Part 1: Tunnels, pp 127–143

Fugeman ICD, Hawley J, Meyers AG (1992) Major underground structures. Proceedings of the Institution of Civil Engineers. The Channel Tunnel, Part 1: Tunnels, pp 87–102

Grimstad E, Barton N (1993) Updating of the Q-system for NMT. In: Kompen R, Opsahl OA, Berg K (eds) Proceedings of the International Symposium on Sprayed Concrete – Modern Use of Wet Mix Sprayed Concrete for Underground Support, Fagernes. Norwegian Concrete Association, Oslo

Makurat A, Barton N, Vik G, Chryssanthakis P, Monsen K (1990) Jointed rock mass modelling. International Symposium on Rock Joints. Loen 1990. Proceedings, pp 647–656

Sharp JC, Warren CD, Barton NR, Mairwood R (1996) In: Harris CS, Hart MB, Varley PM, Warren CD (eds) Fundamental evaluations of the chalk marl for the prediction of UK marine tunnel stability and water inflows. Ch. 32 in Engineering Geology of the Channel Tunnel, pp 472–507

Varley PM, Warren CD (1995) The channel tunnel project. Keynote lecture. GDF bulletin 11. Proc. XIth European Conf. of Soil Mech. and Found. Eng., Copenhagen

Varley PM, Darby A, Radcliffe E (1992) Geology, alignment and survey. Proceedings of the Institution of Civil Engineers. The Channel Tunnel. Part 1: Tunnels, pp 43–54

Warren CD, Varley PM, Parkin R (1992) UK tunnels: geotechnical monitoring and encountered conditions. Ch. 14. Proceedings of the Institution of Civil Engineers. The Channel Tunnel